International Journal of Advance Research in Science and Engineering
Volume No. 11, Issue No. 06, June 2022
www.ijarse.com
IJARSE
ISSN 2319 - 8354

FOG DETECTION AND FREE SPACE SEGMENTATION FOR CAR NAVIGATION USING RESTORATION TECHNIQUE

Gopavarapu Maheswari[1], Bhavanam Sai pujitha[2], Cherukuri. Saran Sai[3], Achanti. Venu Gopi[4],Dr. K. Kanti Kumar[5], Dr. Sk. Ebraheem Khaleelulla[6],

[1,2,3,4]UG Students in Tirumala engineering college, Narasaraopet, Andhra Pradesh, Guntur District -522601
[5]Professor in Tirumala engineering college, Narasaraopet, Andhra Pradesh, Guntur District -522601 [6]Assoc. Professor in Tirumala engineering college, Narasaraopet, Andhra Pradesh, Guntur District -522601

Abstract: During winter season heavy fog occur in morning time, Due to this it is very difficult to identify the object in morning time fog, there is chance of occurring accidents. To overcome from this problem, we are implementing fog detection and free space segmentation for car navigation using Restoration image processing technique. In this technique we can see the objects clearly as it removes the fog from the images grabbed from the vehicle camera. It provides segmented area Fog intensity values are displayed and distance from the object to the original vehicle is Calculated.

Keywords: *Restoration, Free Space Segmentation, fog density, Anomaly route maps.*

1. Introduction

Road path self-supervised technique is one of the tough global Problem withinside the subject of transportation infrastructure. Flat broke avenue floor situations create a chance of harm to cars and will increase probabilities of visitor's accidents. In 2015, the USA Congress surpassed the Surface Transportation Reauthorization and Reform Act for the preservation of federal highways over a five-year duration with a price range of forty-six billion in step with yr. In their survey they referred to that almost 10,000 visitors' fatalities every year [1]. contain terrible avenue situations. Maintaining accurate avenue first-rate is consequently vital now no longer simplest to guide a green avenue community however additionally to lessen Visitor's. Recent Tracking Techniques Global Penetrating Radar (GPR). Different system are used to measure the avenue specific techniques is surveyed. However, this system is costly, costing between $8,000 and $220,000.

2 Methodology

Anomaly detection

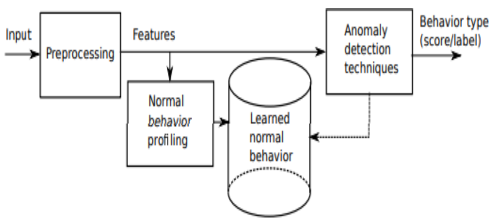

Figure:1. Overview of a typical anomaly detection scheme

Image segmentation

In Image segmentation an image can be divided various sub regions.

- Thresholding
- Edge finding
- Binary mathematical morphology

Gray-value mathematical morphology

2.2.1Thresholding: In thresholding Technique it is based on cut value if the value is greater than one threshold then value is one else the value is zero.

$$\text{If } a[m,n] \geq \theta \quad a[m,n] = object = 1$$
$$\text{Else} \quad a[m,n] = background = 0 \quad \ldots\ldots\ \textbf{Eq (1)}$$

example, If (**Redness {a [m, n]} >= θ**$_{\textbf{red}}$), but the concept is clear.

$$\text{If } a[m,n] < \theta \quad a[m,n] = object = 1$$
$$\text{Else} \quad a[m,n] = background = 0$$

………………… Eq (2)

IJARSE
ISSN 2319 - 8354

Isodata algorithm: This iterative technique for choosing a threshold was developed by Ridler [2] and Calvard. The

histogram is initially segmented into two parts using a starting threshold value such as θ0 = 2B-1, half the maximum dynamic range. Half the maximum dynamic range. The sample mean (mf, 0) of the [3] gray values associated with the foreground pixels and the sample mean (mb, 0) of the gray values associated with the background pixels are computed

$$\theta_k = \left(m_{f,k-1} + m_{b,k-1}\right)/2 \quad until \quad \theta_k = \theta_{k-1}$$

……. Eq (3)

Background-symmetry algorithm- This technique assumes a different and Dominant peak for the foreground that is symmetric about its maximum. The approach can be used smoothing [5] as described. The maximum peak (max(p)) is found by searching for the maximum value in the histogram.

EDGE FINDING

Thresholding provides a segmentation that reproduce all the pixels that, in principle, belong to the things of interest in an image. An alternative to this is to [8] find those pixels that belong to the borders.

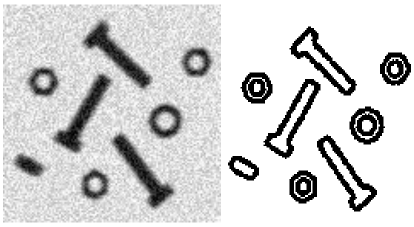

Figure:2 Edge Finding when the value is …………**SNR 30 dB**

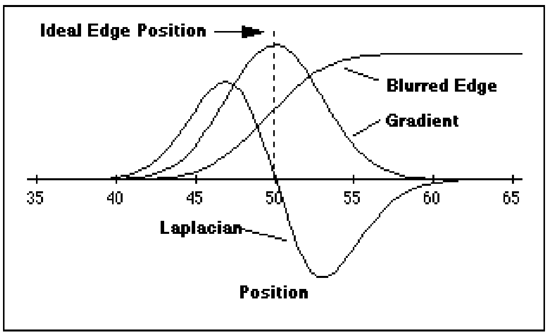

Figure 3: Edge finding based on the Sobel Gradient; equation combined with the Isodata thresholding algorithm

Binary mathematical morphology The various approaches that we have explained for mathematical morphology. I can be puttogether to form best techniques for the processing of binary [4] images and gray level images. As images frequently result from segmentation processes on gray level images, the morphological processing of the image produces result permits the improvement of the segmentation output.

Salt-or-pepper filtering: Segmentation procedures frequently result in isolated "1" pixels in "0" neighbourhood (salt) or isolated "0" pixels in a "1" neighbourhood (pepper)

$$Weights = \begin{bmatrix} w_4 = 16 & w_3 = 8 & w_2 = 4 \\ w_5 = 32 & w_0 = 1 & w_1 = 2 \\ w_6 = 64 & w_7 = 128 & w_8 = 256 \end{bmatrix}$$

Gray-value mathematical morphology

Gray-value morphological processing techniques can be used for practical problems such as shading correction [7]. In this section several other techniques will be presented.

3 Block Diagram

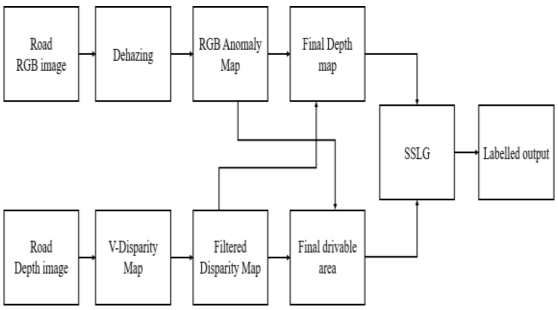

Figure:4. Proposed block diagram.

Dehazing Image It was obtained by using bounding function

delta=zeta./(min_I).^0.5;...... eq(4)

test_tr_proposed= 1./(1 + (MAX.*10.^(-

IJARSE
ISSN 2319 - 8354

0.05*delta))./(A-min_I)); ......eq(5)

Sample images

Figure:4 **Figure:5**

Input Fog Image Defog image

Final-Depth Map

Map Edge detection is a technique of image processing used to identify points in a discontinuity image with dissimilar, simply to say, sharp changes [8] in the image brightness. These points where the image Quality varies sharply are called the edges (or boundaries) of the i

Figure:6 Original RGB Image

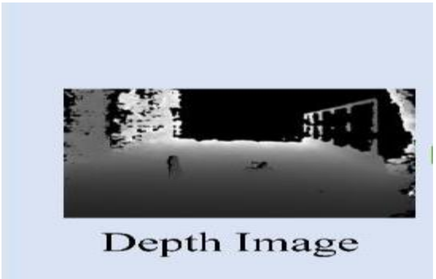

Figure:7 Final Depth map

3.3 V Disparity Map

Gaussian filters are mostly used to reduce noise. Read an image into the workspace. Filter the [10] image with kernel isotropic Gaussian smoothing kernels of increasing standard deviations.

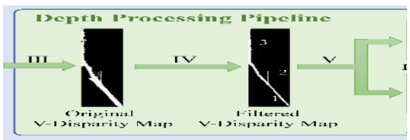

Figure:8 Depth processing

Data Set Collection

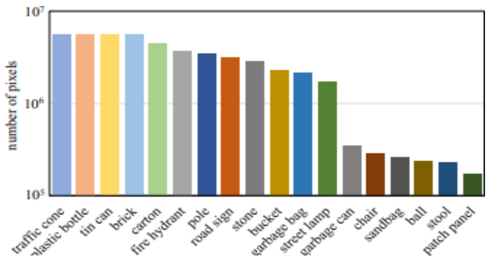

Figure:9 Number of finely annotated pixels (y-axis) and their associated categories (x-axis).

Self-Supervised Label Generator

Our proposed Self-Supervised Label Generator (SSLG) [9] is designed to generate self-supervised labels of drivable areas and road anomalies automatically.

$$U_l = u_l - u_0 = f\frac{X + b/2}{Y\sin\theta + Z\cos\theta}$$ .... Eq (6)

$$U_r = u_r - u_0 = f\frac{X - b/2}{Y\sin\theta + Z\cos\theta}$$ .... Eq (7)

$$V = v - v_0 = f\frac{Y\cos\theta - Z\sin\theta}{Y\sin\theta + Z\cos\theta}$$ ....Eq (8)

$$\Delta = u_l - u_r = f\frac{b}{Y\sin\theta + Z\cos\theta}$$ ....Eq (9)

Horizontal planes in the real-world coordinates can be represented by Y = m, which leads to:

$$\Delta\frac{m}{b} = V\cos\theta + f\sin\theta$$ ......Eq(10)

Similarly, vertical planes in the real-world coordinates can be represented by Z = n, which leads to:

$$\Delta\frac{n}{b} = V\sin\theta + f\cos\theta$$ ......Eq(11)

4.Measurement of Intensity

4.1 PSNR:

Peak signal-to-noise ratio (PSNR) is the ratio between the higher possible power of an image and the power of corresponding unwanted noise quantity that affects the image. To establish the PSNR of an image, it is necessary to compare that image to an ideal clean image with the higher possible power.

International Journal of Advance Research in Science and Engineering
Volume No. 11, Issue No. 06, June 2022
www.ijarse.com
IJARSE
ISSN 2319 - 8354

4.1.1peak signal-to-Noise Ratio

$$PSNR = 10 \cdot \log_{10}\left(\frac{MAX_I^2}{MSE}\right) = 20 \cdot \log_{10}\left(\frac{MAX_I}{\sqrt{MSE}}\right) = 20 \cdot \log_{10}(MAX_I) - 10 \cdot \log_{10}(MSE).$$

……..**Eq(11)**

4.1.2 Mean Square Error

$$MSE = \frac{1}{m\,n}\sum_{i=0}^{m-1}\sum_{j=0}^{n-1}[I(i,j) - K(i,j)]^2.$$

……………………..**Eq(12)**

Estimation of Mean Square Error

Where, O represents the matrix data of original image.
D represents the matrix data of degraded image.
m represents the numbers of rows of pixels and I represent the index of that row of the image.

image. n represents the number of columns of pixels and j represents the index of that column image.
RMSE is the root mean square error.

SSIM Calculation (Structural Similarity Index)

The SSIM Index quality assessment index is based on the computation of three terms, luminance term, contrast term and structural term. [11] The overall index is a multiplicative combination of the three terms.

$$SSIM(x,y) = [l(x,y)]^{\alpha} \cdot [c(x,y)]^{\beta} \cdot [s(x,y)]^{\gamma}$$

where

$$l(x,y) = \frac{2\mu_x\mu_y + C_1}{\mu_x^2 + \mu_y^2 + C_1},$$

$$c(x,y) = \frac{2\sigma_x\sigma_y + C_2}{\sigma_x^2 + \sigma_y^2 + C_2},$$

$$s(x,y) = \frac{\sigma_{xy} + C_3}{\sigma_x\sigma_y + C_3}$$

$$SSIM(x,y) = \frac{(2\mu_x\mu_y + C_1)(2\sigma_{xy} + C_2)}{(\mu_x^2 + \mu_y^2 + C_1)(\sigma_x^2 + \sigma_y^2 + C_2)}$$

……Eq(13)

5. Algorithm

5 .1 Algorithm

Algorithm 1: Original RGB Anomaly Map Generator

Input: $\mathcal{L}$, h, w, σ_s.
Output: $\mathcal{R}_o$.

$\sigma = \min(\mathrm{h}, \mathrm{w})/\sigma_s$
initialize $\mathcal{L}_\omega$ with three channels $(l_\omega, a_\omega, b_\omega)$
construct a Gaussian kernel $\mathcal{G}$ with the size $3\sigma \times 3\sigma$ and the standard deviation σ
$\mathcal{L}_\omega = \mathcal{G}(\mathcal{L})$
$\mathcal{R}_o = \|\mathcal{L} - \mathcal{L}_\omega\|^2$

5.2 Algorithm

Algorithm 2: Final Segmentation Label Generator

```
Input: R_f, D_f, M_D, h, w, κ.
Output: M_L.
compute M_A using (7)
for i ← 1 to h do
    for j ← 1 to w do
        if M_A(i, j) > κ then
            label M_L(i, j) as road anomalies
        else if M_D(i, j) is labeled positive then
            label M_L(i, j) as the drivable area
        else
            label M_L(i, j) as the unknown area
        end
    end
end
```

6 Results and discussion

Dataset: The proposed simulations are implemented on the real time RGB-D dataset. RGB-D cameras, such as the Kinect, are visual sensors that are capable of simultaneously streaming RGB and depth pictures.

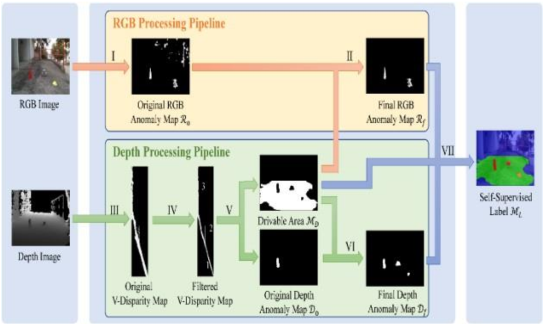

Figure:10

RGB Input Image I, II Original RGB Anomaly Image, III Depth Area Calculation, IV Derivable Area, V, Self-Supervised Area.

6.1 Intensity obtained values

```
PSNR =
    60.5196

MSE
     0.0577

SSIM =
     0.0019
```

Table 1. Performance Comparision

Method	Accuracy	Precision	Recall
EVD [9]	91.785	90.148	90.160
RSL [11]	92.233	92.482	91.622
DSL [13]	94.161	95.005	92.116
Propsoed method	97.651	96.644	92.544

7 Conclusion

In this work, we presented a comprehensive study on the drivable area and road anomaly segmentation problem for robotic wheelchairs. A self-supervised approach was proposed, which contains an automatic labelling pipeline for drivable area and road anomaly segmentation. Experimental results showed that our proposed automatic labelling pipeline achieved an impressive speed-up compared to manual labelling. In addition, the project "FOG DETECTION AND FREE SPACE SEGMENTATION FOR CAR NAVIGATION USING RESTORATION TECHNIQUE" is successfully implemented and tested by using MATLAB 2016 Here the proposed system identify the objects clearly during morning time fog, It provides derivable Area, It display the intensity Values, Finally It provides the distance from object to the vehicle.

8. REFERENCES

[[1].Z. Zhang, "Microsoft Kinect sensor and its effect," IEEE multimedia, vol. 19, no. 2, pp. 4–10, 2012.
[2] Y. Sun, M. Liu, and M. Q.-H. Meng, "Active Perception for Foreground Segmentation: An RGB-D Data-Based Background Modeling Method," IEEE Transactions on Automation Science and Engineering, pp. 1–14, 2019.
[3] "Motion removal for reliable rgb-d slam in dynamic environments," Robotics and Autonomous Systems, vol. 108, pp. 115 – 128, 2018.
[4] "Improving rgb-d slam in dynamic environments: A motion removal approach," Robotics and Autonomous Systems, vol. 89, pp. 110 – 122, 2017.
[5] C. Hazira's, L. Ma, C. Domokos, and D. Cremer's, "Fuse net: Incorporating depth into semantic segmentation via fusion-based cnn architecture," in Asian Conference on Computer Vision. Springer, 2016, pp. 213–228.
[6] W. Wang and U. Neumann, "Depth-aware cnn for rgb-d segmentation," in The European Conference on Computer Vision (ECCV), September 2018.
[7] F. Lateef and Y. Ruichek, "Survey on semantic segmentation using deep learning techniques," Neurocomputing, 2019.
[8] R. Labayrade, D. Aubert, and J.-P.Tarel, "Real time obstacle detection in stereovision on non-flat road geometry through" v-disparity" representation," in Intelligent Vehicle Symposium, 2002. IEEE, vol. 2. IEEE, 2002, pp. 646–651.
[9] Y. Gao, X. Ai, Y. Wang, J. Rarity, and N. Dahnoun, "uv-disparity based obstacle detection with 3d camera and steerable filter," in Intelligent Vehicles Symposium (IV), 2011 IEEE. IEEE, 2011, pp. 957–962.
[10] Y. Cong, J.-J. Peng, J. Sun, L.-L. Zhu, and Y.-D. Tang, "V-disparity based ugv obstacle detection in rough outdoor terrain," Acta Automatica Sinica, vol. 36, no. 5, pp. 667–673, 2010.
[11] D. Yiruo, W. Wenjia, and K. Yukihiro, "Complex ground plane detection based on v-disparity map in off-road environment," in

Intelligent Vehicles Symposium (IV), 2013 IEEE. IEEE, 2013, pp. 1137–1142.